PRAMANA
—journal of
physics

© Printed in India

Vol. 50, No. 4,
April 1998
pp. 271–280

Correlation between zeroes and poles of S matrix for complex potentials

I JAMIR, E F P LYNGDOH and C S SHASTRY
Department of Physics, North Eastern Hill University, Shillong 793 022, India

MS received 6 October 1997; revised 13 March 1998

Abstract. Using several illustrative examples, the nature of resonance poles and the corresponding zeroes of the s-wave S matrix is examined for several potentials having an absorptive pocket followed by a barrier. It is shown that even though the presence of absorption practically suppresses the manifestation of resonance in the elastic scattering cross section, the effect of the resonances generated by the absorptive pocket is more clearly manifested in the absorption cross section provided the barrier width is not too large. We further find that the signature of barrier top resonances are also more clearly manifested in the absorption cross section rather than in the elastic scattering cross section. These results have been interpreted in terms of complex resonance poles and corresponding zeroes of the S matrix. This implies that in complex potential scattering like heavy ion collisions, the reaction channel cross section peak is a more reliable signature of resonance phenomenon than the variation of the elastic channel cross section with energy.

Keywords. S-matrix; resonance.

PACS Nos 24.90; 03.65

1. Introduction

The analytic properties of the S matrix for real well-behaved potentials, their applications in scattering theory and the interpretation of physical states of quantal systems, are well-established subjects [1–3]. However, in nuclear scattering, the effective potential between the interacting systems is complex and detailed investigations and applications of the analytic properties of the S matrix for complex nuclear potentials have been studied only to a limited extent [4–7]. Recently, there has been some renewed interest in the nature of the singularities of the S matrix for complex potentials and its applications to nuclear physics [8–11]. It may be noted that in complex potential scattering, the primary observables of interest are the scattering cross section σ_s and the absorption cross section σ_{ab}. It is desirable to study to what extent both of these quantities can be correlated with the analytic features and poles of the S matrix.

In this connection, we note that the poles of the S matrix in the complex energy plane with positive real part and small negative imaginary part can be correlated with resonance states of energy E_R and width Γ [1]. These poles are obtained from the study of the s-wave S matrix as a ratio of the Jost functions $f(k)$ and $f(-k)$,

$$S(k) = \frac{f(k)}{f(-k)}.$$

We use the convention $2m = \hbar = 1$ and energy $E = k^2$. In numerical calculations, we express energy in fm^{-2} unit and length in fm. The Jost functions $f(\pm k)$ are defined as the Wronskian $W[\phi(k,r), f(\pm k,r)] = f(\pm k)$ where $\phi(k,r)$ is the regular solution of the modified radial Schrödinger equation with potential $U(r)$,

$$\frac{\mathrm{d}^2\phi(r)}{\mathrm{d}r^2} + [k^2 - U(r)]\phi(r) = 0 \tag{1}$$

having the behaviour $\phi(r) \simeq r$ near the origin and the Jost solutions $f(\pm k,r)$ of eq. (1) behave as $\text{Lt}_{r\to\infty} \exp(\pm ikr) f(\pm k,r) = 1$. Some authors, as a matter of convention use the symbol $f(-k)$ for $f(k)$ and vice versa (for example, see refs [1] and [8]).

For real potentials, the Jost functions satisfy the symmetry relations $f^*(k) = f(-k^*)$ which means that for real $k, f^*(k) = f(-k)$. We denote any typical pole position in the k-plane by k_P and the corresponding zero by k_Z. The analytic properties of $f(k)$ ensures that if $k_P = \text{Re}(k_P) - i\ \text{Im}(k_P)$ is a zero of $f(-k)$, then the corresponding zero of $f(k)$ is $k_Z = k_P^*$. This makes the distribution of the poles and corresponding zeroes of the S matrix symmetric with respect to the real k axis. For potentials with a pocket, resonance states occur inside the pocket which can decay by tunneling through the barrier between the outer region and the pocket. For large barrier parameters, the imaginary part of the resonance poles become exceedingly small and this can lead to very sharp and narrow resonances implying that extremely high resolution is needed to resolve them. However, when an absorptive complex potential

$$U(r) = U_0 g(r) \tag{2}$$

with U_0 complex having $\text{Im}(U_0) < 0$ and form factor $g(r)$ is used, the symmetry relation of the Jost function changes [4] to $f^*(k, U_0) = f(-k^*, U_0^*)$. As a result, the zeroes and poles of the S matrix are no longer symmetrically distributed with respect to the real k axis. Hence, we cannot conclude that there is a zero of the S matrix at $k = k_P^*$ corresponding to a pole at $k = k_P$. Further, resonance states inside the pocket can have larger widths of the order of $\text{Im}\,(U_0)$ or larger and hence can give significantly broader resonances. It is therefore important to see to what extent such resonances get manifested in σ_s and σ_{ab} as a function of energy. In the case of complex potential scattering, the zeroes of the S matrix have additional significance due to the fact that σ_{ab} is governed by the factor $(1 - |S(k)|^2)$. This means that one can expect σ_{ab} to have a maximum when $|S(k)|$ is a minimum. This minimum can be expected to occur in the vicinity of the complex zero of the S matrix. Thus peaks in σ_{ab} are related in this sense to the zeroes of the S matrix.

This raises the question as to whether the resonance poles which should get manifested in σ_s (which gets suppressed due to the large $\text{Im}\,(k_P)$) can be related to the peaks in σ_{ab} which occur due to the zeroes of the S matrix. Such a clear correlation can come only when $\text{Re}\,(k_P)$ and the corresponding $\text{Re}\,(k_Z)$ are same or very close to each other. In this paper, we examine this problem using several examples and demonstrate that even though the peaks in σ_s get suppressed due to the presence of the complex potential, the presence of these states are manifested in σ_{ab} at about the same energies when the imaginary part

of the poles and zero position in energy plane are reasonably well separated. This is because the real part of the resonance poles and the corresponding zeroes are found to be very close to each other in the energy plane. This means that it is appropriate to look forward to the nature of the resonance states by studying the peaks of the absorption cross section as a function of energy. In § 2, we describe the details of our calculation and § 3 gives the discussion and conclusion.

2. Resonance poles and zeroes of S matrix for complex potentials

In this section we calculate the zeroes and poles of the s-wave S matrix for three different absorptive potentials having a barrier in the outer region. Such potentials can generate resonance states of comparatively large widths inside the potential pocket. We then examine the variation of σ_s and σ_{ab} as a function of E and interpret them in terms of the poles and zeroes of the S matrix.

2.1 *Rectangular barrier with absorptive pocket*

We first study the poles and zeroes of the S matrix of the potential

$$\begin{aligned} U(r) &= -iW, \quad r < a \\ &= U_B, \quad a \leq r \leq b \\ &= 0, \quad r > b \end{aligned} \tag{3}$$

with $U_B = 8\,\text{fm}^{-2}$, $W = 0.2\,\text{fm}^{-2}$, $a = 5\,\text{fm}$, $b = 5.5\,\text{fm}$. This gives an absorptive pocket in the region $r < a$, followed by a barrier of height U_B and width $(b - a)$. The s-wave S matrix is obtained analytically by solving the radial Schrödinger equation which is straightforward and we omit the algebraic details. The poles and zeroes of the S-matrix are calculated using Newton–Raphson iterative procedure. In figure 1a, we show the variation of σ_s and σ_{ab} for s-wave as a function of energy. Curve B indicates σ_s obtained with $W = 0$, i.e. curves C and B indicate the scattering cross section in the presence and absence of absorption inside the potential pocket. The minima of σ_s are very small but non-zero. The minima in σ_s are due to the variation of the hard core type phase shift present in the S matrix and are not intimately correlated with resonance. Figure 1b shows the resonance poles and corresponding zeroes in the E-plane. Table 1 lists the location of the same poles and zeroes in the k-plane. The points in the upper (lower) half k^2-plane in figure 1b should be understood to belong to the first (second) Riemann sheet. Same observation holds for figure 2b and figure 3b described later.

It is clear that the introduction of the imaginary part in the potential practically eliminates the sharp resonances of curve B from curve C. It should be understood that the broad peaks in σ_s are not the state resonances but arise as shape resonances. We also note that the location of the peaks in curve A are practically at the position of the peaks in curve B. The corresponding peaks in curve C are unable to manifest itself due to the large width arising from the complex potential.

From figure 1b it is clear that the imaginary part of the pole is close to or greater than W. It is also interesting to note that for the sharpest resonance corresponding to the

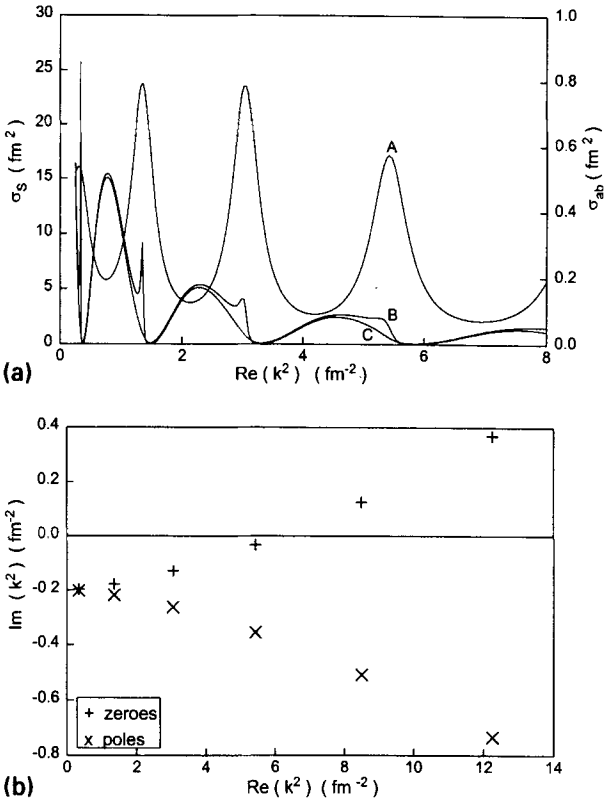

Figure 1. (**a**) Variation of σ_s and σ_{ab} with energy for the rectangular barrier of eq. (3) with $U_B = 8\,\text{fm}^{-2}$, $W = 0.2\,\text{fm}^{-2}$, $a = 5$ fm and $b = 5.5$ fm. Curve A is the plot of σ_{ab} and curves C and B correspond to σ_s with and without absorption respectively. (**b**) Position of poles and zeroes corresponding to curves A and C in the k^2 plane. When poles and zeroes lie very close to each other, the marker resembles an asterisk.

Table 1. Poles and zeroes of the S matrix in k plane for the rectangular barrier of eq. (3).

$U_B = 8\ \text{fm}^{-2}$, $a = 5$ fm, $b = 5.5$ fm

Poles		Zeroes	
$W = 0$	$W = 0.2\ \text{fm}^{-2}$	$W = 0$	$W = 0.2\ \text{fm}^{-2}$
$0.582\text{-}2.100 \times 10^{-3}i$	$0.605\text{-}0.167i$	$0.582 + 2.100 \times 10^{-3}i$	$0.605\text{-}0.163i$
$1.642\text{-}8.461 \times 10^{-3}i$	$1.671\text{-}9.332 \times 10^{-2}i$	$1.642 + 8.461 \times 10^{-3}i$	$1.675\text{-}7.641 \times 10^{-2}i$
$1.747\text{-}1.922 \times 10^{-2}i$	$1.747\text{-}7.535 \times 10^{-2}i$	$1.747 + 1.922 \times 10^{-2}i$	$1.748\text{-}3.691 \times 10^{-2}i$
$2.330\text{-}3.452 \times 10^{-2}i$	$2.329\text{-}7.614 \times 10^{-2}i$	$2.330 + 3.451 \times 10^{-2}i$	$2.331\text{-}7.119 \times 10^{-3}i$
$2.915\text{-}5.444 \times 10^{-2}i$	$2.914\text{-}8.735 \times 10^{-2}i$	$2.915 + 5.444 \times 10^{-2}i$	$2.916 + 2.151 \times 10^{-2}i$
$3.500\text{-}7.908 \times 10^{-2}i$	$3.499\text{-}0.106i$	$3.500 + 7.908 \times 10^{-2}i$	$3.501 + 5.197 \times 10^{-2}i$

bottom of the pocket, the S matrix pole and zero are located very close to each other and they gradually diverge as far as the imaginary part is concerned, as the real part of the poles and zeroes in the energy plane increases. Thus, one can state that peaks in σ_{ab}

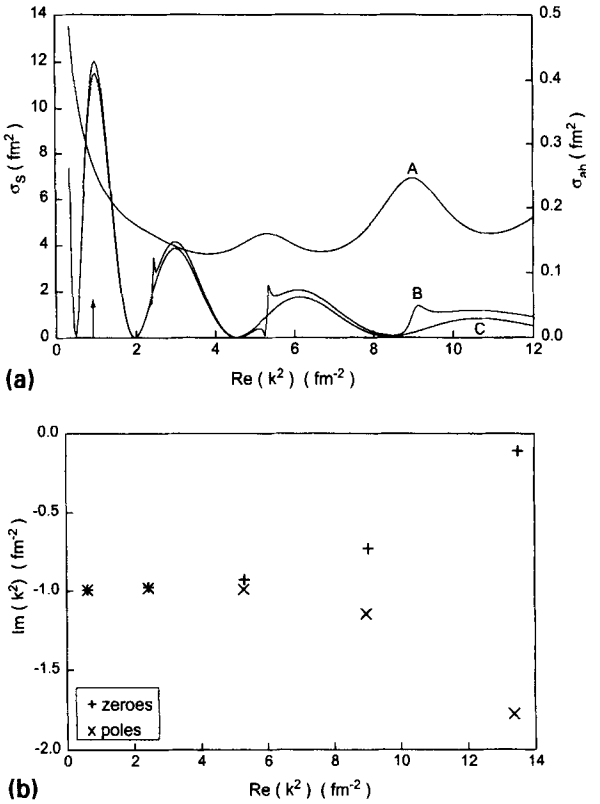

Figure 2. (**a**) Variation of σ_s and σ_{ab} with energy for the Gaussian barrier of eq. (4) with $U_B = 10\,\text{fm}^{-2}$, $W = 1\,\text{fm}^{-2}$, $a = 0.5\,\text{fm}$, $a_I = 0.3\,\text{fm}$, $R_G = 4.25\,\text{fm}$ and $R = 4.25\,\text{fm}$. Curve A is the plot of σ_{ab} and curves C and B correspond to σ_s with and without absorption respectively. The arrow mark indicate the position of the first extremely narrow peak in curve B which have not been reproduced due to the finite step size of the energy intervals. (**b**) Same as figure 1b for the potential of eq. (4).

indicate the presence of resonance states generated by the complex potential. The conclusion is, non-elastic or reaction channels provide a much clearer signature of resonance than the corresponding elastic channel. Figure 1a also indicates that the width of the σ_s resonance peaks in curve B gradually increases as the real part of the energy becomes large as it should since $\Gamma \propto \text{Im}\,(E_R)$. Physically speaking, this means that a resonance state with higher energy can decay more easily by tunneling across the barrier as compared to the states with lower energy. The conclusion from figures 1a and 1b is that peaks in σ_{ab} arise from the zeroes of the S matrix but at the same time indicate resonance state positions because the real part of zeroes and poles for these cases are practically the same as indicated in figure 1b. The first peak in σ_{ab} at $k^2 \simeq 0.6\,\text{fm}^{-2}$ is less prominent because in this case, the S matrix pole and zero having appreciable imaginary parts are very close to each other thus making $|S(k) \simeq 1|$. This point will be elaborated later.

Table 2. Poles and zeroes of the S matrix for the Gaussian barrier with absorptive pocket of eq. (5).

$U_B = 10\,\text{fm}^{-2}$, $R_G = 4.25\,\text{fm}, R = 4.25\,\text{fm}$, $a = 0.5\,\text{fm}$, $a_I = 0.3\,\text{fm}$

Poles		Zeroes	
$W = 0\,\text{fm}^{-2}$	$W = 1\,\text{fm}^{-2}$	$W = 0\,\text{fm}^{-2}$	$W = 1\,\text{fm}^{-2}$
$0.787\text{-}0.416 \times 10^{-4}i$	$0.946\text{-}0.525i$	$0.788 + 1.416 \times 10^{-4}i$	$0.946\text{-}0.525i$
$1.561\text{-}1.128 \times 10^{-3}i$	$1.591\text{-}0.309i$	$1.561 + 1.128 \times 10^{-3}i$	$1.591\text{-}0.307i$
$2.303\text{-}6.975 \times 10^{-3}i$	$2.312\text{-}0.214i$	$2.303 + 6.975 \times 10^{-3}i$	$2.314\text{-}0.201i$
$3.001\text{-}3.520 \times 10^{-2}i$	$3.001\text{-}0.191i$	$3.001 + 3.520 \times 10^{-2}i$	$3.008\text{-}0.121i$
$3.668\text{-}0.113i$	$3.664\text{-}0.242i$	$3.668 + 0.113i$	$3.676\text{-}1.510 \times 10^{-2}i$

2.2 *Gaussian barrier with absorptive pocket*

Now, we examine the same problem for a smoother potential having a Gaussian barrier with an absorptive Woods–Saxon pocket

$$U(r) = U_B \exp\left[-\left(\frac{r - R_G}{a}\right)^2\right] - iW\left[1 + \exp\left(\frac{r - R}{a_I}\right)\right]^{-1} \tag{4}$$

with $U_B = 10\,\text{fm}^{-2}$, $W = 1\,\text{fm}^{-2}$, $R_G = 4.25\,\text{fm}$, $R = 4.25\,\text{fm}$, $a = 0.5\,\text{fm}$, $a_I = 0.3\,\text{fm}$. In this example, the barrier is comparatively broader. We have solved the Schrödinger equation using the Runge–Kutta method and the results of the calculation are summarized in figures 2a, b and table 2. We see that this potential essentially reproduces results that corroborate those of the previous potential, given by (3) leading to similar conclusions. We note that the sharp resonance peaks in σ_s in curve B for $W = 0$ gradually gets narrower ($\simeq 10^{-4}\,\text{fm}^{-2}$) until they are too narrow to be observed due to the finite size of the energy steps used for the calculation. The arrow in figure 2a indicates the position of the sharpest resonance of curve B. But as in the previous example, the locations of these extremely sharp peaks match with the positions of the corresponding absorption peaks for the higher lying states. This point is explained in § 3. Compared with the former case, this potential has a larger imaginary part and width and the absorption cross section shows less structure as compared with that in figure 1a. Numerically speaking, this is due to the fact that poles and zeroes of the S matrix for this complex potential are much closer to each other than the corresponding case depicted in figure 1b. In this case, barrier tunneling is reduced due to the larger width and higher barrier. As expected, in the present case the resonance peaks in σ_s for $W = 0$ are sharper than the previous case studied.

2.3 *Woods–Saxon type barrier with absorptive pocket*

As the last example, we analyse the potential having a still larger barrier with a Woods–Saxon shape and an absorptive pocket of the same shape [11]. This potential is given by

$$U(r) = U_B\left[1 + \exp\left(\frac{R_0 - c_1 - r}{a_1}\right)\right]^{-1} - iW\left[1 + \exp\left(\frac{r - R_0 + c_W}{a_W}\right)\right]^{-1}, \quad r < R_0 \tag{5}$$

$$U(r)=U_B\left[1+\exp\left(\frac{r-R_0-c_2}{a_2}\right)\right]^{-1}-iW\left[1+\exp\left(\frac{r-R_0+c_W}{a_W}\right)\right]^{-1},\quad r>R_0.$$

The parameters used for this potential are $U_B = 10\,\mathrm{fm}^{-2}$, $W = 1\,\mathrm{fm}^{-2}$, $R_0 = 4.5\,\mathrm{fm}$, $a_1 = 0.12\,\mathrm{fm}$, $a_2 = 0.25\,\mathrm{fm}$, $a_W = 0.05\,\mathrm{fm}$, $c_1 = 1.5\,\mathrm{fm}$, $c_2 = 2\,\mathrm{fm}$, $c_W = 1.5\,\mathrm{fm}$. The scattering and absorption cross sections as well as the positions of the poles and zeroes given in figures 3a, b and table 3 at first glance, do not seem to be similar to our previous two potentials of (3) and (4). The large barrier width effectively suppresses tunneling though the barrier and the corresponding resonances in curve B with $W = 0$ have extremely narrow widths. These peaks in curve B have not been reproduced in the graph due to the finite step size of the energy interval but we have indicated them by arrow marks. We have verified that these fine peaks in σ_s are reproduced with discernible width

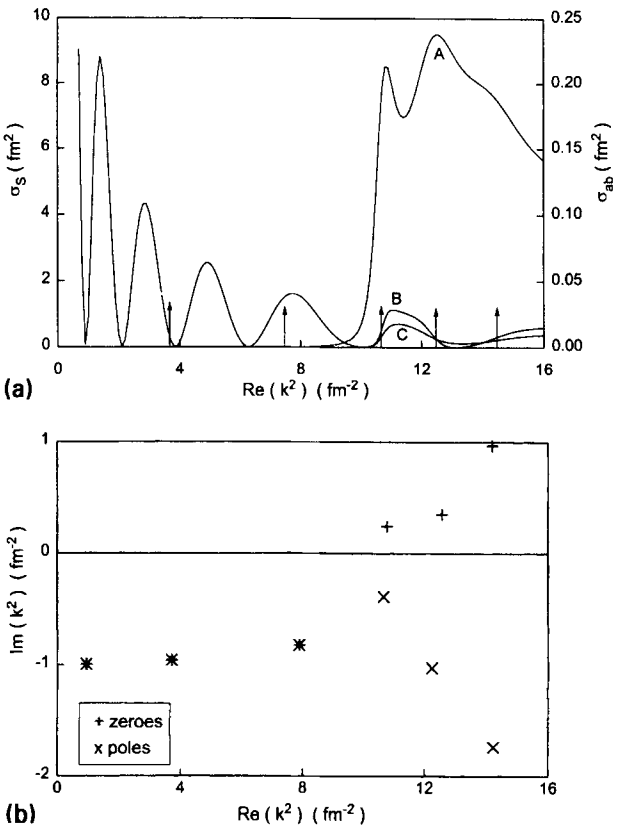

Figure 3. (**a**) Variation of σ_s and σ_{ab} with energy for the Woods–Saxon shaped barrier of eq. (5) with $U_B = 10\,\mathrm{fm}^{-2}$, $W = 1\,\mathrm{fm}^{-2}$, $a_1 = 0.12\,\mathrm{fm}$, $a_2 = 0.25\,\mathrm{fm}$, $a_W = 0.05\,\mathrm{fm}$, $c_1 = 1.5\,\mathrm{fm}$, $c_2 = 2\,\mathrm{fm}$, $c_W = 1.5\,\mathrm{fm}$, $R_0 = 4.5\,\mathrm{fm}$. Curve A is the plot of σ_{ab} and curves C and B correspond to σ_s with and without absorption respectively. The arrow marks indicate the positions of the extremely narrow peaks in curve B which have not been reproduced due to the finite step size of the energy intervals. Below $E = 10\,\mathrm{fm}^{-2}$, curves B and C practically merge into one. (**b**) Same as figure 1b for the potential of eq. (5).

Table 3. Poles and zeroes of the S matrix for the Woods–Saxon shape barrier with absorptive pocket of eq. (6).

$U_B = 10\,\text{fm}^{-2}$, $R_G = 4.5\,\text{fm}$, $a_1 = 0.12\,\text{fm}$, $a_2 = 0.25\,\text{fm}$, $a_W = 0.05\,\text{fm}$, $c_1 = 1.5\,\text{fm}$, $c_2 = 2.0\,\text{fm}$, $c_W = 1.5\,\text{fm}$

Poles		Zeroes	
$W = 0\,\text{fm}^{-2}$	$W = 1\,\text{fm}^{-2}$	$W = 0\,\text{fm}^{-2}$	$W = 1\,\text{fm}^{-2}$
$0.978\text{-}3.244 \times 10^{-11}i$	$1.081\text{-}0.459i$	$0.978 + 3.286 \times 10^{-11}i$	$1.081\text{-}0.459i$
$1.928\text{-}7.743 \times 10^{-9}i$	$1.945\text{-}0.246i$	$1.928 + 7.743 \times 10^{-9}i$	$1.945\text{-}0.246i$
$2.808\text{-}2.274 \times 10^{-5}i$	$2.815\text{-}0.146i$	$2.808 + 2.274 \times 10^{-5}i$	$2.815\text{-}0.146i$
$3.275\text{-}4.774 \times 10^{-2}i$	$3.267\text{-}5.976 \times 10^{-2}i$	$3.275 + 4.774 \times 10^{-2}i$	$3.283 + 3.719 \times 10^{-2}i$
$3.518\text{-}9.981 \times 10^{-2}i$	$3.504\text{-}0.147i$	$3.518 + 9.981 \times 10^{-2}i$	$3.545 + 5.013 \times 10^{-2}i$
$3.779\text{-}0.180i$	$3.779\text{-}0.229i$	$3.779 + 0.180i$	$3.771 + 0.128i$

if the width of the barrier is decreased. More importantly, the display of the zeroes and poles of the S matrix does not show the symmetry in the E-plane which was present in the earlier two examples. This indicates that the symmetry in figures 1b and 2b should not be considered as the general feature of the zeroes and poles of the S matrix for complex potentials. However, one feature which may be noted is that as far as the deeper lying resonances are concerned, both the zeroes and poles practically coincide with each other. In such cases, peaks in σ_{ab} also are not observed. The nature of variation of poles and zeroes in figure 3b shows the dramatic difference between below barrier absorptive pocket resonances and above barrier resonances. The above barrier resonances in this case are very clearly manifested in σ_{ab} but not in σ_s. It may be mentioned here that the resonances in heavy ion scattering which have highly absorptive pocket followed by large Coulomb barrier are often associated with barrier region orbiting resonance states.

3. Discussion and conclusions

We further analyse our results as follows. In the case of real potential we have $\text{Re}(k_P) = \text{Re}(k_Z)$ and in the examples studied, we find that the same relation is valid to a good degree of accuracy for complex absorptive potentials. Since the poles are observed to occur lower down in the k-plane as compared to the corresponding zeroes, the following relations also hold for complex potentials.

$$\text{Im}(k_Z) > \text{Im}(k_P) \quad \text{and} \quad |\text{Im}(k_P)| > |\text{Im}(k_Z)|.$$

For the s-wave scattering case, we have

$$\sigma_s = \frac{\pi}{k^2}|1 - S(k)|^2,$$

$$\sigma_{ab} = \frac{\pi}{k^2}(1 - |S(k)|^2).$$

Near a pole or zero, we can write the S matrix as

$$S(k) = g(k)\frac{k - k_Z}{k - k_P},$$

where we assume $g(k)$ is a shape function that varies very slowly with k in the vicinity of a pole. Setting $\mathrm{Re}\,(g) \approx 1$ and $\mathrm{Im}\,(g) \approx 0$ in the neighbourhood of a pole, we get

$$\frac{\mathrm{d}}{\mathrm{d}k}|S(k)|^2 = 0 \quad \text{and} \quad \frac{\mathrm{d}^2}{\mathrm{d}k^2}|S(k)|^2 > 0 \text{ at } k = \mathrm{Re}\,(k_P)$$

and hence $S(k)$ has a minimum at $k = \mathrm{Re}\,(k_P)$. This will give rise to a maximum in the absorption cross section at the same energy. However, the corresponding rise in the scattering cross section is suppressed by the imaginary part of the potential due to the fact that in this case,

$$|1 - S(k)|^2 = \left(1 - \frac{\mathrm{Im}\,(k_Z)}{\mathrm{Im}\,(k_P)}\right)^2$$

and for all cases, either $\mathrm{Im}\,(k_Z) \simeq \mathrm{Im}\,(k_P)$ or $|\,\mathrm{Im}\,(k_Z)| < |\,\mathrm{Im}\,(k_P)|$. Hence $|1 - S(k)|^2$ becomes much smaller than the maximum possible value 4. On the other hand, in the case of real potentials, $|1 - S(k)|^2 = 4$ near a resonance. Thus the lack of mirror symmetry with respect to the real k axis and the nature of the poles and zeroes for complex potentials suppresses the resonance peaks in σ_s which the corresponding real potential can manifest when proper resolution is taken.

The width ΔE of the absorption peak of $(1 - |S(k)|^2)$ can be shown to be $\Delta E \simeq 4|\,\mathrm{Re}\,(k_P)\,\mathrm{Im}\,(k_P)|$. Even though a similar relation is valid for the peak in σ_s, due to the drastic suppression of the peak height as explained above, these are suppressed in σ_s.

As seen earlier in the case of the potential given by eq. (5), there are no peaks in σ_{ab} observed at lower energies because in this region, the complex zeroes and poles having significant imaginary parts are practically same leading to $|S(k)| \simeq 1$ for $E = E_R$. This can also be interpreted in terms of the inhibition posed by the large barrier to generate absorption in the pocket at lower energies. Thus in general, the variation of σ_{ab} provides a better indicator of the *effective* resonances in complex potentials as compared to σ_s.

To summarize, we have examined the poles and zeroes of the S matrix for three typical complex potentials having absorptive pocket followed by a barrier. We find that in general, the real parts of the low lying zeroes and the corresponding poles of $S(k)$ are practically the same and the imaginary parts are significantly different either in sign or magnitude or both. Such a statement is also substantially true for higher poles and zeroes. Due to this, $|1 - S(k)|^2$ gets greatly suppressed as compared with its peak value $(= 4)$ and hence elastic channel resonance peaks are not manifested appreciably. On the other hand, the zeroes of the S matrix corresponding to a pole enhance the absorption cross section factor $(1 - |S(k)|^2)$ in the vicinity of resonance energies. This enhancement prominently occurs when $|\,\mathrm{Im}\,(k_P)|$ is significantly larger than $|\,\mathrm{Im}\,(k_Z)|$ but when $\mathrm{Im}\,(k_P)$ is quite close to $\mathrm{Im}(k_Z)$, even in σ_{ab} the peaks get eliminated. As a result, peaks in σ_{ab} can be correlated with the resonances generated by the complex potential. This is consistent with the fact that in the analysis of resonances in nucleus-nucleus collisions, one of the important criteria for identifying resonance is that resonance structure should appear correlated in energy in several exit i.e., reaction channels. [12] The peaks in the absorption cross section also gets suppressed if the width of the barrier is quite large and in such cases, peaks in σ_{ab} occur due to the barrier top states. These observations mean that in

complex potential scattering having pockets with large absorption, only the states around the barrier top may manifest clearly as peaks in σ_{ab} and the corresponding peaks in σ_s will be comparatively weaker.

References

[1] R G Newton, in *Scattering Theory of Waves and Particles* (McGraw-Hill, New York, 1966) p. 339
[2] V de Alfaro and T Regge, in *Potential Scattering* (North-Holland, Amsterdam, 1975) p. 34
[3] C J Jochain, in *Quantum Collision Theory* (North-Holland, Amsterdam, 1965) p. 243
[4] S Mukherjee and C S Shastry, *Nucl. Phys.* **A128**, 256 (1969)
[5] S Joffily, *Nucl. Phys.* **A215**, 301 (1973)
[6] L P Kok and H van Haeringa, *Ann. Phys. (NY)* **131**, 426 (1981)
[7] W Cassing, M Stingl and A Weiguny, *Phys. Rev.* **C26**, 22 (1982)
[8] J Dabrowski, *Phys. Rev.* **C53**, 2004 (1996)
[9] A Gal, G Toker and Y Alexander, *Ann. Phys. (NY)* **137**, 341 (1981)
[10] E Oset, P F de Córdoba, L L Salcedo and R Brockman, *Phys. Rep.* **188**, 79 (1990)
[11] P Susan, B Sahu, B M Jyrwa and C S Shastry, *J. Phys.* **G20**, 1243 (1994)
[12] R Singh in *Nuclear Reactions* edited by R Singh and S N Mukherjee (New Age International Limited 1996) p. 206